STUB BASED EQUIVALENT CIRCUIT MODELS FOR EVEN/ODD MODE DUAL CRLH UNIT CELLS

Amr M. E. Safwat[1, *], Amr A. Ibrahim[1], Mohamed A. Othman[2], Marwah Shafee[1], and Tamer M. Abuelfadl[2]

[1]Electronics and Electrical Communication Engineering Department, Faculty of Engineering, Ain Shams University, Cairo, Egypt

[2] Electronics and Electrical Communication Engineering Department, Faculty of Engineering, Cairo University, Giza, Egypt

Abstract—The theory of even/odd mode based dual composite right/left handed (D-CRLH) unit cells is developed, and a unified modeling approach based on stubs is presented. The theory shows that these unit cells will have left-handed behavior if the even and odd mode corresponding stubs have dual behavior. Several unit cells are investigated. The proposed models agree with EM simulations. Experimental results confirm the presented theory.

1. INTRODUCTION

Left-handed (LH) transmission line (TLs) have led to a wealth of novel applications [1–3]. Practically, they are realized using commercial off-the-shelf components, distributed components, or both [4, 5]. Due to physical constraints, the LH bands are always accompanied with right-handed (RH) bands. Hence, they are called composite right/left handed (CRLH) TLs.

Recently, the authors have proposed several unit cells that have D-CRLH behavior, i.e., the RH band appears before the LH one as explained in [4] and shown in Fig. 1. In [6], it was shown that a unit cell that consists of series short-circuited stub and shunt open-circuited stub posses D-CRLH behavior. In that unit cell, the LH band was extremely small and it was very difficult to achieve the balance condition due to the difference between the propagation velocities in the two stubs. A better alternative was the microstrip meandered

(a)   (b)

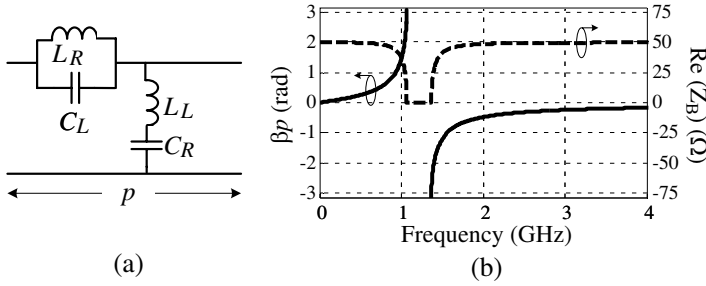**Figure 1.** Dual CRLH unit cell [4]. (a) Circuit schematic. (b) Dispersion relation and Bloch impedance ($L_R = 3.3\,\mathrm{nH}$, $C_R = 1.32\,\mathrm{pF}$, $L_L = 13.2\,\mathrm{nH}$, $C_L = 5.28\,\mathrm{pF}$).

coupled-lines [7, 8]. The odd and even modes behave as series short-circuited and shunt open-circuited stubs, respectively, and they have approximately the same propagation velocities. Hence, a large LH band was obtained. The same behavior was observed in slotted microstrip open-circuited shunt stub [9], coplanar waveguide (CPW) open-circuited shunt stubs [10], and ring-shaped microstrip coupled lines [11].

In this paper, the theory that links the operation of these unit cells is developed, three novel structures are presented, and stub-based equivalent circuit models are proposed. Theory is confirmed by EM simulations and measurements. The proposed theory can be used to quickly assess the performance of coupled line based CRLH unit cells and to determine their LH and RH regions. Compared to conventional lumped-element model [12–15], the proposed model operates over wide band and considers the distributed nature of the unit cells. Furthermore, such simple theory will pave the way to come up with new CRLH unit cells shapes with compact sizes. The paper is organized as follows: in Section 2 the theory is presented, proposed stub-based equivalent circuit models are shown in Section 3 along with new CRLH unit cells shapes, and the conclusion is drawn in Section 4.

2. EVEN AND ODD ANALYSIS OF SYMMETRIC UNIT CELLS

A simple way to analyze a symmetric circuit is to use the H/E-symmetry plane analysis, as shown in Fig. 2(a). Using this technique the circuit is characterized by the even and odd input impedances, denoted by Z_{in}^{even} and Z_{in}^{odd}, respectively, and the parameters of the
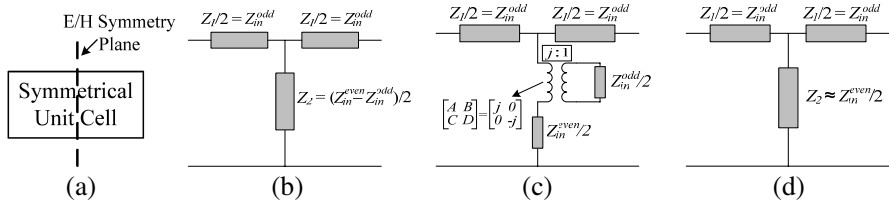
Figure 2. Symmetrical unit cell. (a) E-plane/H-plane. (b) T model in terms of Z_{in}^{odd} and Z_{in}^{even}. (c) Exact model. (d) Approximate model when Z_{in}^{odd} tends to zero.

equivalent T-network, shown in Fig. 2(b), are written as follows:

$$Z_1 = 2Z_{in}^{odd} \tag{1}$$

$$Z_2 = \left(Z_{in}^{even} - Z_{in}^{odd} \right)/2 \tag{2}$$

The negative sign in the shunt branch can be modeled by a fictitious transformer that has imaginary turn ratio ($j : 1$). Its equivalent $ABCD$ matrix presentation is shown in Fig. 2(c). If Z_{in}^{odd} is relatively small, the equivalent circuit model will reduce to the simplified one shown in Fig. 2(d). This condition will be shown to be valid for most of the unit cells discussed in this paper around the balance frequency.

If this circuit, the circuit in Fig. 2(b), is used as a unit cell in a periodic structure, the propagation factor and Bloch impedance will be [16],

$$\cos(\beta d) = \frac{Z_{in}^{even} + Z_{in}^{odd}}{Z_{in}^{even} - Z_{in}^{odd}} \tag{3}$$

$$Z_B = \sqrt{Z_{in}^{even} Z_{in}^{odd}} \tag{4}$$

To have a propagation passband, (4) requires that Z_{in}^{even} and Z_{in}^{odd} are out of phase. For passive circuits this condition reduces to Z_{in}^{even} is capacitive and Z_{in}^{odd} is inductive, or vice versa. The former condition corresponds to RH behavior with phase and group velocities in the same direction, while the second case corresponds to LH behavior with opposite phase and group velocities.

In the next section, this simple modeling approach is used to study several unit cells that are symmetric and, moreover, support two electrical modes.

3. STUB BASED EQUIVALENT CIRCUIT MODELS

3.1. Microstrip Slotted Open-circuited Shunt Stub

This unit cell, which was proposed in [9], is shown in Fig. 3(a). It consists of a host microstrip line symmetrically loaded by slotted microstrip shunt stubs (microstrip cross transition). Due to the presence of the slot symmetrically beneath the stub, two electrical modes that have even and odd mode symmetry are present. In [9], a transformer based equivalent circuit model was developed. The model, which is shown in Fig. 3(b), was capable to separate between the even and odd modes, and it was shown that the even mode behaves as an open-circuited stub while the odd mode behaves as a short-circuited stub.

To get better insights, a simple stub based model can be derived by applying the modeling approach presented in the previous section.
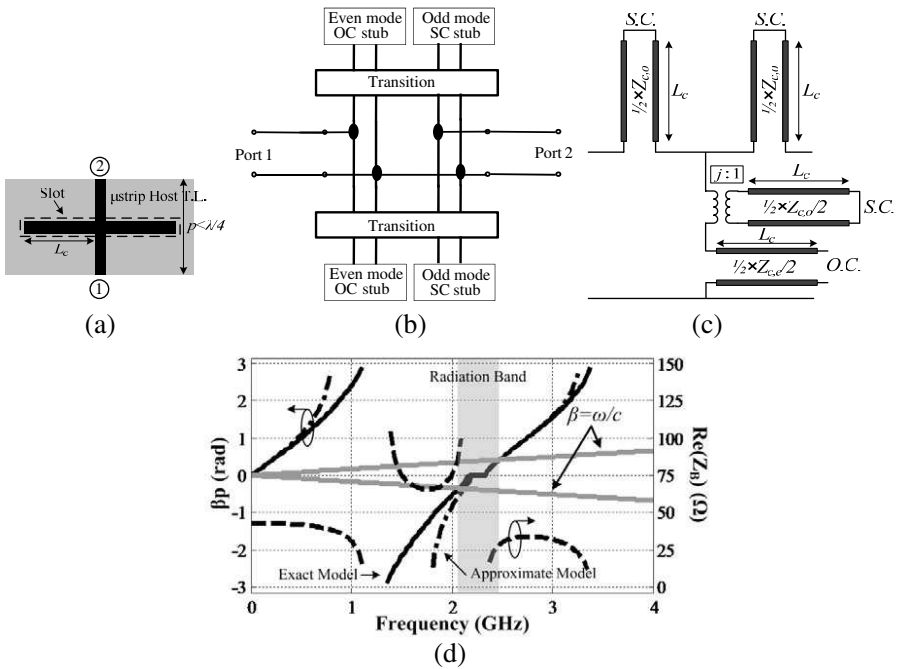

Figure 3. Slotted microstrip stub. (a) Schematic. (b) Mode-based equivalent circuit model. (c) Stub-based equivalent circuit model. (d) Dispersion relation.

Fig. 3(c) shows the resultant model, where

$$Z_{in}^{even} = -jZ_{c,e}\cot(\beta_e L), \quad Z_{in}^{odd} = jZ_{c,o}\tan(\beta_o L) \tag{5}$$

$Z_{c,e}$, $Z_{c,o}$ are the characteristic impedances, and β_e, β_o are the propagation constants of the even and odd modes, respectively. The factor half in the model results from the fact that the stubs are connected symmetrically to the host line.

If this circuit is employed as a unit cell in a periodic structure and assuming that $\beta_e \approx \beta_o$, the phases of Z_{in}^{even} and Z_{in}^{odd} are always opposite, indicating all pass characteristic. Starting at low frequencies Z_{in}^{even} is purely capacitive and Z_{in}^{odd} is inductive giving a RH behavior. However, when the electrical lengths of the stubs exceed $\pi/2$, Z_{in}^{even} becomes inductive and Z_{in}^{odd} becomes capacitive resulting in LH behavior.

For a host line with 2.8 mm width and 10 mm length, strip and slot with 2 mm width and 33 mm length, and a substrate with $\varepsilon_r = 4.4$ and $h = 1.6$ mm, the equivalent electrical parameters are as follows: the host line has $50\,\Omega$ characteristic impedance and 3.3 effective dielectric constant, and the even and odd modes have $67\,\Omega$ and $120\,\Omega$ characteristic impedances and 3.1 and 2.3 effective dielectric constants, respectively. The corresponding dispersion diagram extracted from the stub based circuit model is shown in Fig. 3(d). The first band is RH. Beyond the first transition frequency, which occurs at 1.2 GHz, the performance switches to LH. At the balance frequency, the second transition frequency at 2.4 GHz, the transmission line restores its RH performance.

Near the balance frequency, Z_{in}^{odd} tends to zero, hence the stub based model can be simplified to the one shown in Fig. 2(d). In the series branch the odd mode behaves as a short-circuited series stub, while in the shunt branch the even mode behaves as an open-circuited shunt stub. The dispersion relation using this simplified model is also depicted in Fig. 3(d). Accurate and simplified models agree near the balance frequency, while they deviate at the first transition frequency from RH to LH.

Six unit cells are cascaded to implement a dual-CRLH microstrip line. Both conductor and dielectric losses are neglected in the circuit and EM simulations. However, radiation losses are included in the EM simulations only as the structure is surrounded by a radiation sphere. EM and circuit simulations, shown in Fig. 4, agree well except around the balance frequency. This is expected since radiation occurs within this region. Also, there is a slight frequency shift between the circuit and EM simulations, which is due to the dispersive nature of the slotline, not considered in the circuit simulations.
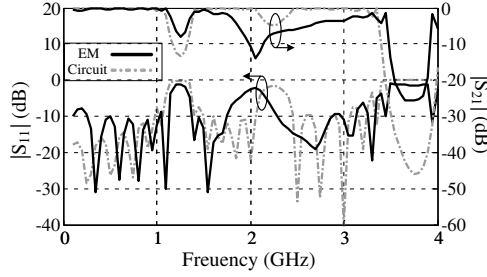
Figure 4. Circuit versus EM simulations of six cascaded slotted microstrip stub D-CRLH cells [9].

The proposed structure was fabricated on FR4 (h = 1.6 mm, $\varepsilon_r = 4.4$, and $\tan \delta = 0.02$). Measurements and EM simulations were in a very good agreement as was shown in [9].

3.2. CPW Open-circuited Shunt Stub

The same procedure can be applied to the CPW open-circuited shunt stub shown in Fig. 5(a). The host line, due to symmetry, has one propagating mode, the even mode, while the stub, due to the absence of air-bridges, has two electrical modes, even and odd. The stub-based equivalent circuit model is identical to the one shown in Fig. 3(c). For host CPW that has 3 mm width, 0.3 mm gap separation and 10.6 mm pitch length, open-circuited shunt stub that has 1 mm width, 0.3 mm separation and 34 mm length, and substrate that has $\varepsilon_r = 4.4$ and height (h) = 1.6 mm, the equivalent electrical parameters
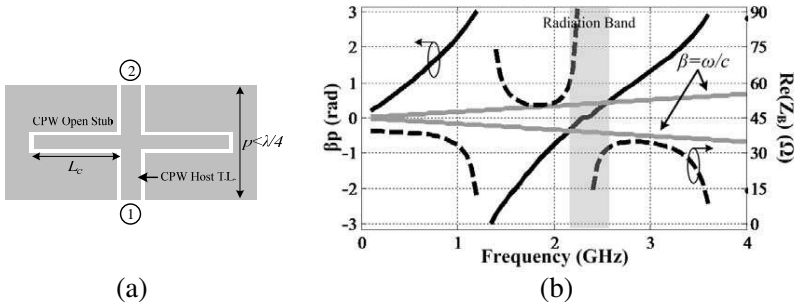

Figure 5. CPW open-circuited shunt stub. (a) Schematic. (b) Dispersion relation.

are as follows: the host line has $50\,\Omega$ characteristic impedance and 2.46 effective dielectric constant, and the even and odd modes of the CPW stubs have $59\,\Omega$ and $110\,\Omega$ characteristic impedances and 2.6 and 2.2 effective dielectric constants, respectively. The corresponding dispersion relation is shown in Fig. 5(b). Similar to the slotted-microstrip stub, the CPW open circuited shunt stub has dual CRLH behavior. The first transition frequency occurs at 1.2 GHz, while the balance frequency, transition from LH to RH band, occurs at 2.4 GHz.

In [10], a transformer based equivalent circuit model was derived, and it was shown that the stub CPW even mode behaves as open-circuited stub and the stub CPW odd mode behaves as short-circuited stub. It was also shown why air-bridges were needed to eliminate the LH behavior. Moreover, this metamaterial-inspired interpretation was shown to be capable to explain why the angle of peak radiation varies from backward to forward direction as the frequency varies from LH band to RH band.
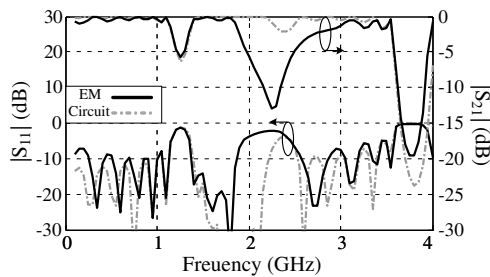

Figure 6. Circuit versus EM simulations of six cascaded CPW open-circuited shunt stubs [10].

Figure 6 shows the circuit and EM simulations of six cascaded CPW open-circuited shunt stubs. As expected from theory, stopband occurs at the first transition frequency, 1.2 GHz, while radiation occurs near the balance frequency, 2.4 GHz. In [10], the structure was fabricated on FR4. Both S-parameters and radiation characteristics were measured and they were in good agreement with simulations.

3.3. Microstrip Meander Coupled Lines

The same even and odd mode conditions exist in the microstrip meander coupled lines proposed in [7] and shown in Fig. 7(a). They, also, have the same stub-based equivalent circuit model, shown Fig. 3(b). The dispersion relation, which corresponds to host line of width 3.9 mm, coupled lines of separation 0.5 mm, length 40 mm, width
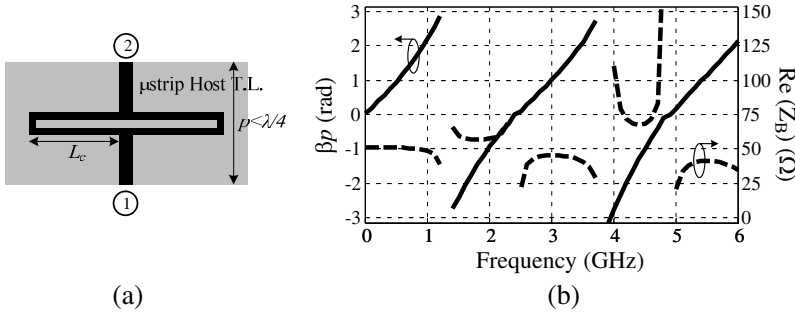
(a)   (b)

Figure 7. Meander coupled line unit cell. (a) Schematic. (b) Dispersion relation.

1mm, and pitch 8 mm, on a substrate of height 1.6 mm, and $\varepsilon_r = 2.33$, is shown in Fig. 7(b). It is similar to those of the microstrip slotted stub and CPW open-circuited shunt stub.

Seven cells are cascaded to form a D-CRLH. Circuit simulations and EM simulations, shown in Fig. 8, are in a very good agreement. Measurements extracted from [7], are also shown in Fig. 8. They agree very well with theoretical results.
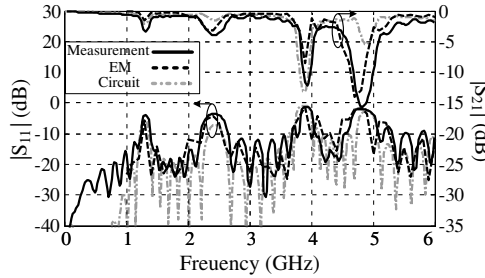

Figure 8. Microstrip meander coupled line D-CRLH, measurements versus simulations (Circuits and EM) [7].

3.4. Microstrip Ring-shaped Coupled Lines

Ring-shaped coupled lines, shown in Fig. 9, also posses LH behavior. In [11], twelve coupled line topologies were investigated theoretically, and it was shown that the closed and opened loops possess LH behavior. Unfortunately, geometrical models did not provide a physical understanding for this behavior. Also, transformer-based models and
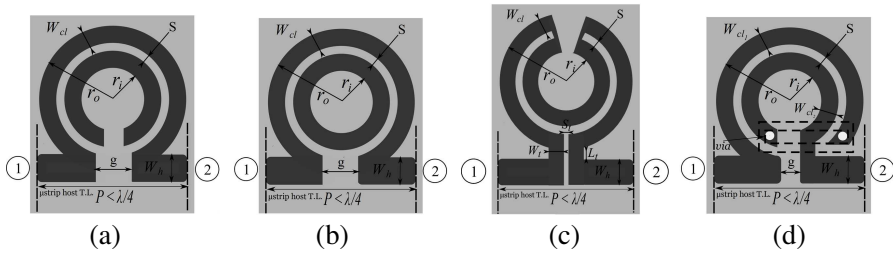
Figure 9. Ring-shaped microstrip coupled-lines. (a) Open loop: $W_{cl} = 1.2$ mm, $S = 0.5$ mm, $p = 14$ mm, $r_i = 5.1$ mm, $r_o = 6.8$ mm, $W_h = 1.5$ mm, $g = 0.6$ mm, and $L_c = 37.4$ mm. (b) Closed loop: $W_{cl} = 2.1$ mm, $S = 6$ mm, $p = 14.4$ mm, $r_i = 6$ mm, $r_o = 9$ mm, $W_h = 1.5$ mm, $g = 0.6$ mm, and $L_c = 36$ mm. (c) Crescent shaped: $W_{cl} = 3.5$ mm, $S = 0.5$ mm, $p = 12.2$ mm, $r_i = 3.7$ mm, $r_o = 11.2$ mm, $W_h = 4.7$ mm, $W_t = 3.5$ mm, $L_t = 2.34$ mm, $S_t = 0.5$ mm, and $L_c = 30.6$ mm. (d) Diagonally connected: $r_o = 3.8$ mm, $r_i = 1.3$ mm, $S = 0.6$ mm, $W_{cl1} = 1.1$ mm, $W_{cl2} = 1.9$ mm, $g = 0.7$ mm, $L_c = 18.3$ mm, and $p = 7.4$ mm.

the segregation between even and odd modes, as presented in [9, 10], are not feasible for these structures.

Applying the E/H symmetry plane analysis on the closed loop, Fig. 9(a), reveals that Z_{in}^{even} and Z_{in}^{odd}, shown in Fig. 10(a), are given by:

$$Z_{in}^{even} = -j\frac{Z_{c,e}}{2}\cot\left(\beta_e\frac{L_c}{2}\right) - j\frac{Z_{c,o}}{2}\cot\left(\beta_o\frac{L_c}{2}\right) \qquad (6a)$$

$$Z_{in}^{odd} = j2Z_{c,e}\tan\left(\beta_e\frac{L_c}{2}\right)//j2Z_{c,o}\tan\left(\beta_o\frac{L_c}{2}\right) \qquad (6b)$$

i.e., Z_{in}^{even} consists of two open-circuited stubs connected in series, while Z_{in}^{odd} consists of two short-circuited stubs connected in shunt. Each stub has a length of $L_c/2$ where L_c is the average circumference of the rings. It is clear that Z_{in}^{even} is capacitive starting from DC till the electrical length of the stubs ($L_c/2$) exceeds $\pi/2$ where it becomes inductive. On the other hand, Z_{in}^{odd} has exactly the dual performance. Thus, the first LH-RH transition will occur when L_c corresponds to λ_g. The same analysis method can be applied to the open loop structure shown in Fig. 9(b) and the resulting Z_{in}^{even} and Z_{in}^{odd} are shown in Fig. 10(b). The performance of this structure can be assessed similarly to the closed loop one. Both structures have D-CRLH as shown in the dispersion relation depicted in Figs. 11(a) and (b), respectively.
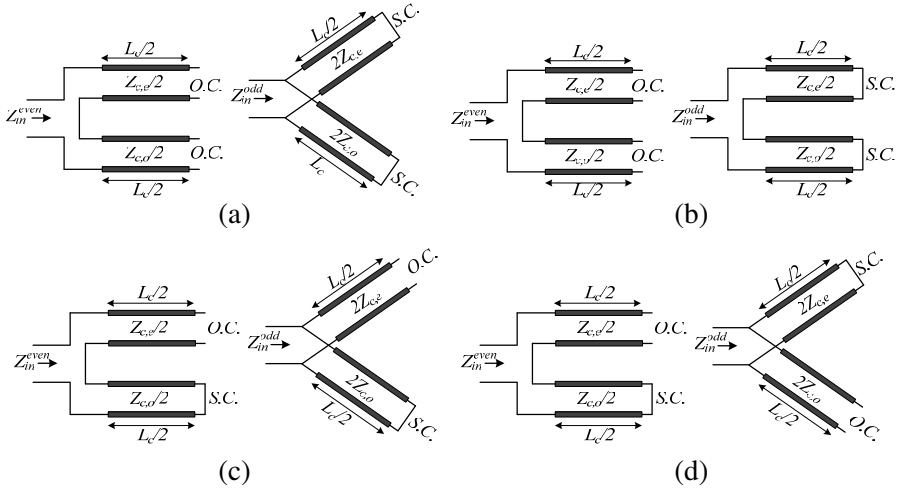
Figure 10. Z_{in}^{even} and Z_{in}^{odd} of ring-shaped unit cells: (a) closed loop, (b) open loop, (c) crescent-shaped, and (c) diagonally connected.
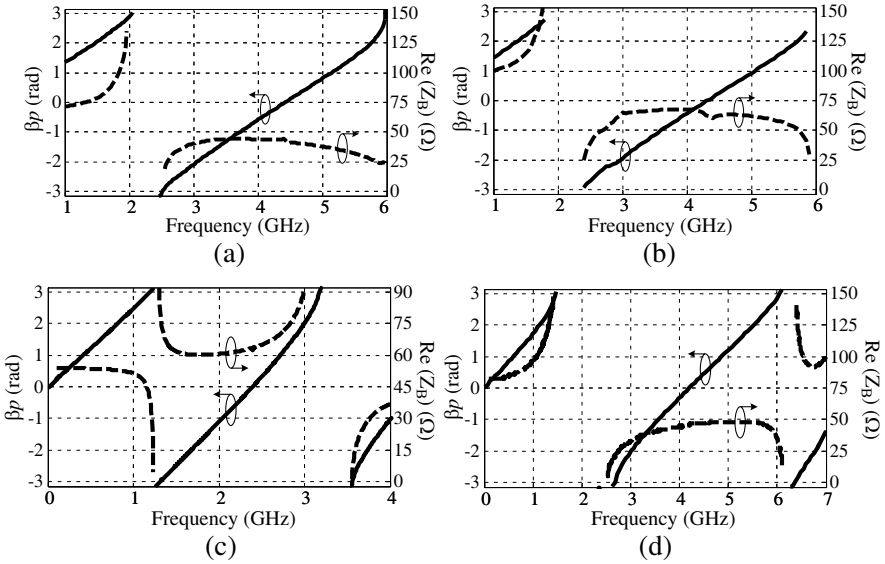

Figure 11. Dispersion relation of ring-shaped microstrip coupled-lines: (a) closed loop, (b) open loop, (c) crescent-shaped, and (d) diagonally connected.

This stub-based model can be intuitively obtained using the following simple procedure: to determine Z_{in}^{even}, the network is evenly excited and an H-plane is inserted at the plane of symmetry. The terminations seen by the even and odd modes of the coupled lines at the symmetry plane determine whether the corresponding stub is short circuited or open circuited, while the termination at the terminal that is next to the input determines whether the two stubs are connected in series or in parallel. If it is short circuited, then the two stubs are connected in parallel, and if it is open circuited then the two stubs are connected in series. The same steps are followed to calculate Z_{in}^{odd} but with E-symmetry plane instead of H-symmetry plane. It should be noted that care must be taken when differentiating between the E/H excitations of the unit cell and the even/odd modes of the coupled lines.

This proposed modeling approach paves the way to new compact-sized ring-shaped D-CRLH unit cells, e.g., the crescent-shaped D-CRLH unit cell shown in Fig. 9(c). Under both the E/H symmetry planes, the even mode of the coupled lines will always see an open circuit (resulting in an open-circuited stub), while the odd mode of the coupled lines will always see a short circuit (resulting in a short-circuited stub). However, these two stubs are connected in shunt/series under the E/H symmetry conditions resulting in the $Z_{in}^{odd}/Z_{in}^{even}$ shown in Fig. 10(c). This is because the terminal next to the input is short/open circuited under the E/H symmetry conditions. It can be shown easily that for this unit cell, Z_{in}^{even} will be capacitive at low frequency, then changes to be inductive when the electrical length of the stubs ($L_c/2$) corresponds to $\pi/8$. Thus, the balance frequency of this unit cell will occurs when L_c corresponds to $\lambda_g/2$. Hence, this unit cell will occupy nearly half the area of the open loop (or closed loop) unit cell for the same balance frequency. The dispersion relation of this unit cell is depicted in Fig. 11(c) where the balance frequency is designed to be around 2.4 GHz.

The stub modeling approach can also be used to study coupled lines cells with symmetry points, rather than symmetry planes, e.g., the diagonally connected coupled lines unit cell proposed in [9] and shown in Fig. 9(d). Connections can be realized with air-bridges, however, due to the limited resources, they are realized through vias connected to a patch patterned in the ground. In this case Z_{in}^{even} and Z_{in}^{odd} are written as:

$$Z_{in}^{even} = -j\frac{Z_{c,e}}{2}\cot\left(\beta_e\frac{L_c}{2}\right) + j\frac{Z_{c,o}}{2}\tan\left(\beta_o\frac{L_c}{2}\right) \tag{7a}$$

$$Z_{in}^{odd} = j2Z_{c,e}\tan\left(\beta_e\frac{L_c}{2}\right) // -j2Z_{c,o}\cot\left(\beta_o\frac{L_c}{2}\right) \tag{7b}$$

which are modeled as shown in Fig. 10(d). The equivalent stub model for this diagonally connected unit cell is very similar to that of the crescent-shaped unit cell and it can be shown that its balance frequency also corresponds to $L_c = \lambda_g/2$. It is interesting to note that although the crescent shaped unit cell and the diagonally connected unit cell are topologically different, they have similar electrical performance as evident from their equivalent stub model.

The four cells have been implemented in five-unit D-CRLH TLs. They are fabricated on Rogers RT/duroid 5870 substrate ($\varepsilon_r = 2.33$ and $h = 1.6\,\text{mm}$). Picture of the fabricated structures are shown in Fig. 12. All dimensions are shown in Fig. 9. Fig. 13 shows the

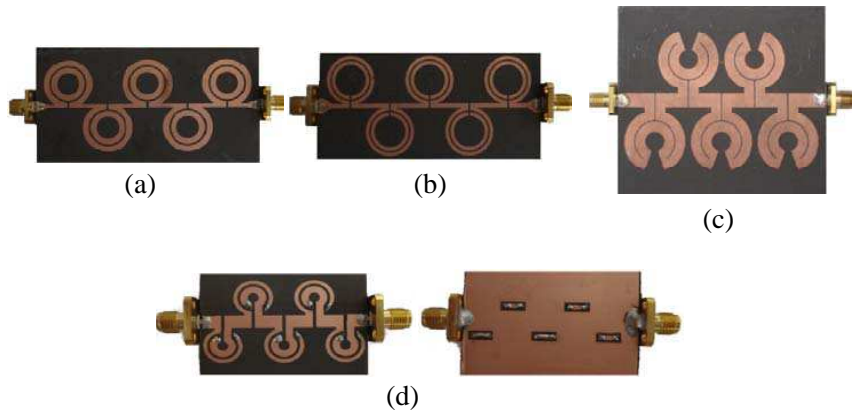(a)   (b)

(c)

(d)

Figure 12. Picture of the fabricated ring-shaped D-CRLH TLs: (a) closed loop, (b) open loop, (c) crescent shape, and (d) diagonally connected.

Table 1. Lateral dimensions comparison for different unit cells.

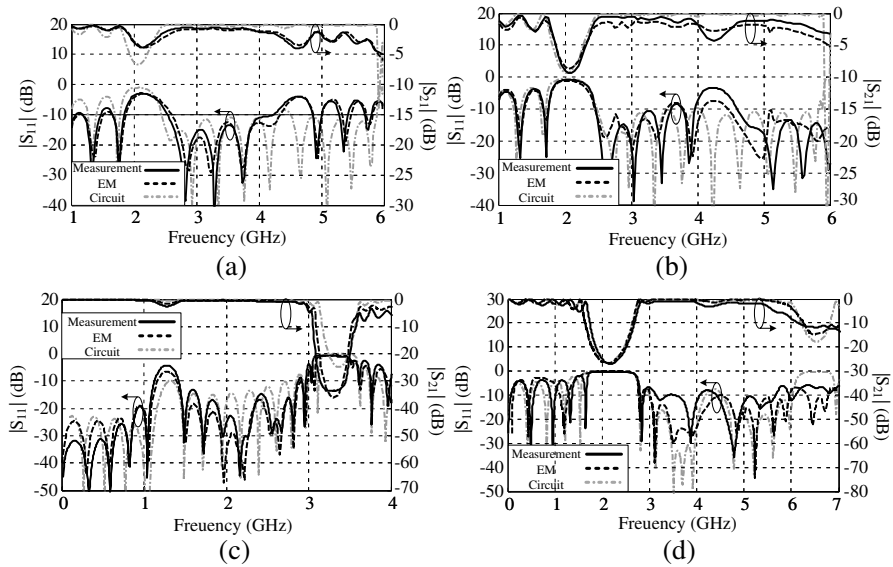| Unit Cell	Lateral Dimension in Terms of λ_g at the First Balance Frequency
Slotted microstrip stubs	0.5
CPW open stubs	0.5
Microstrip coupled lines	0.5
Open loop	0.25
Closed loop	0.32
Crescent shape	0.29
Diagonally connected	0.16

Figure 13. Measurements versus simulations of ring-shaped microstrip coupled line D-CRLH: (a) closed loop, (b) open loop, (c) crescent-shaped, and (d) diagonally connected.

measured, and circuit and EM simulated return and insertion losses. Results are in a very good agreement. The balance frequency occurs at 4.2 GHz as originally designed except for the crescent-shaped unit cell where the balance occurs at 2.4 GHz. The stopbands at the balance frequency are smaller than the straight stubs.

Table 1 shows the lateral dimensions of all cells in terms of the guided wavelength at the balance frequency. Ring-shaped cells have smaller size than straight stubs. Diagonally-connected cells have the smallest size. Crescent-shaped cells should occupy the same size as the diagonally connected. However, due to fabrication limitation of the coupled line width and separation, they have larger size.

4. CONCLUSION

Theory of even/odd mode based D-CRLH unit cells was proposed. The equivalent circuit models reveal that the two electrical modes, though they occupy the same space, have dual-stub behavior, which allows the generation of LH bands. Several D-CRLH unit cells were studied. Theoretical results were compared to experimental data, and they were in a very good agreement.

The proposed theory provides a metamaterial inspired interpretation for the operation of conventional devices, e.g., meandered coupled lines and CPW open circuited shunt stubs. It allows the design of novel D-CRLH, e.g., slotted microstrip open-circuited shunt stubs, opened and closed loop microstrip coupled lines. It also provides design guideline to compact size vias-less D-CRLH unit cells, e.g., crescent-shaped microstrip coupled lines.

REFERENCES

1. Caloz, C. and T. Itoh, *Electromagnetic Metamaterials: Transmission Line Theory and Microwave Applications*, Wiley, New York, 2006.

2. Engheta, N. and R. W. Ziolkowski, *Metamaterials: Physics and Engineering Explorations*, Wiley-IEEE Press, New York, 2006.

3. Eleftheriades, G. and K. Balmain, *Negative-refraction Metamaterials: Fundamental Principles and Applications*, Wiley, New York, 2005.

4. Caloz, C., "Dual composite right/left-handed (D-CRLH) transmission line metamaterial," *IEEE Microw. Wireless Compon. Lett.*, Vol. 16, No. 11, 585–587, Nov. 2006.

5. Eleftheriades, G. V., "A generalized negative-refractive-index transmission-line (NRI-TL) metamaterial for dual-band and quad-band applications," *IEEE Microw. Wireless Compon. Lett.*, Vol. 17, No. 6, 415–417, Jun. 2007.

6. Safwat, A. M. E., "High impedance wire composite right/left-handed transmission lines," *Microwave and Optical Technology Letters*, Vol. 52, 1390–1393, 2010.

7. Safwat, A. M. E., "Microstrip coupled line composite right/left-handed unit cell," *IEEE Microw. Wireless Compon. Lett.*, Vol. 19, No. 7, 434–436, Jul. 2009.

8. Fouda, A., A. M. E. Safwat, and H. El-Hennawy, "On the applications of the coupled line composite right/left-handed unit cell," *IEEE Trans. Microw. Theory and Tech.*, Vol. 58, No. 6, 1584–1591, Jun. 2010.

9. Othman, M. A., A. D. Alwakil, M. Shafee, T. Abuelfadl, and A. M. E. Safwat, "Novel even/odd mode-based CRLH unit cells based," *IEEE MTT-S Int. Microw. Symp. Dig.*, 1–4, 2011.

10. Alwakil, A. and A. M. E. Safwat, "Left-handed behavior of coplanar waveguide open-circuited shunt stub," *IEEE Microw. Wireless Compon. Lett.*, Vol. 22, No. 6, 306–308, Jun. 2012.

11. Safwat, A. M. E. and T. M. Abuelfadl, "Coupled lines from filter to composite right/left handed cells," *Progress In Electromagnetics Research B*, Vol. 26, 451–469, 2010.

12. Esteban, J., C. Camacho-Peñalosa, J. Page, and T. Martın-Guerrero, "Generalized lattice network-based balanced composite right-/left-handed transmission lines," *IEEE Trans. Microw. Theory and Tech.*, Vol. 60, No. 8, 2385–2393, Aug. 2012.

13. Durán-Sindreu, M., G. Sisó, J. Bonache, and F. Martín, "Planar multi-band microwave components based on the generalized composite right/left handed transmission line concept," *IEEE Trans. Microw. Theory and Tech.*, Vol. 58, No. 12, 3382–3391, Dec. 2010.

14. Baena, J. D., J. Bonache, F. Martin, R. Sillero, F. Falcone, T. Lopetegi, M. Laso, J. Garcia-Garcia, I. Gil, I., M. Portillo, and M. Sorolla, "Equivalent-circuit models for split-ring resonators and complementary split-ring resonators coupled to planar transmission lines," *IEEE Trans. Microw. Theory Tech.*, Vol. 53, No. 4, 1451–1461, Apr. 2005.

15. Shamonin, M., E. Shamonina, V. Kalinin, and L. Solymar, "Resonant frequencies of a split ring resonator: Analytical solutions and numerical simulations," *Microw. Opt. Technol. Lett.*, Vol. 44, No. 1, 133–136, Jan. 2005.

16. Collin, R. E., *Foundations for Microwave Engineering*, 2nd edition, Wiley-IEEE Press, 2000.